European Journal of Pharmaceutical Sciences 170 (2022) 106108

Contents lists available at ScienceDirect

European Journal of Pharmaceutical Sciences

journal homepage: www.elsevier.com/locate/ejps

Nebulization of a polyelectrolyte-drug system for systemic hypertension treatment

Nazareth E. Ceschan [a,b,*], Sebastián Scioli-Montoto [c], María Laura Sbaraglini [c], María Esperanza Ruiz [c], Hugh D.C. Smyth [d], Verónica Bucalá [a,e], María V. Ramírez-Rigo [a,b]

[a] Planta Piloto de Ingeniería Química (PLAPIQUI), CONICET – Universidad Nacional del Sur (UNS), Camino La Carrindanga km 7, 8000 Bahía Blanca, Argentina
[b] Departamento de Biología, Bioquímica y Farmacia, UNS, San Juan 670, 8000 Bahía, Blanca, Argentina
[c] Laboratory of Bioactive Research and Development (LIDeB), Faculty of Exact Sciences, Universidad Nacional de La Plata (UNLP)
[d] College of Pharmacy, The University of Texas at Austin, 2409 West University Avenue, Austin, TX, United States
[e] Departamento de Ingeniería Química, UNS, Avenida Alem 1253, 8000 Bahía, Blanca, Argentina

ARTICLE INFO

Keywords:
Polyelectrolyte-drug formulation
Aerosolization behavior
Cell viability
Mucoadhesiveness
Pharmacokinetics

ABSTRACT

Hypertension is a chronic pathology where blood pressure levels are continuously high, causing cardiac, renal, cerebral, and vascular damage leading to early morbi-mortality. This illness is the main risk factor for cardiovascular diseases and the main cause of atrial fibrillation. Atenolol (AT) is a β-1 blocker drug useful for antihypertension and antiarrhythmic treatments. However, this drug possesses low oral bioavailability associated to its low permeability and extensive hepatic first-pass metabolism. To solve the conventional AT-administration problems, oral controlled-release and transdermal delivery have been reported. In this work, an alternative AT inhalatory system administered by nebulization is presented. This system is based on an ionic complex between acidic groups of alginic acid and cationic groups of AT (AA-AT), which was obtained by spray-drying. Pharmaceutical and biopharmaceutical properties for AA-AT inhalatory administration using a jet nebulizer were investigated. The aerodynamic performance (assayed at different cup-nebulizer loadings) of the nebulized system demonstrated that around 40% of the formulation would deposit in the respiratory membrane, with mass median aerodynamic diameters of 3.4–3.6 μm. The AT carried in the AA-AT system was released adequately by ionic exchange in saline solution by permeation through a cellulose membrane. The presence of AA as polyelectrolyte conferred mucoadhesive properties to the ionic complex. Even at high relative AA-AT concentrations, no cytotoxic effect was detected in A-549 cell line. Finally, the preliminary pharmacokinetic assay in the in vivo model confirmed that AT was absorbed from the lung to the systemic circulation, with a greater plasmatic AUC compared to the pure drug (around 50% higher). Then, the system and the nebulization administration demonstrated potential for drug cardiac targeting.

1. Introduction

Cardiovascular diseases are the main cause of dead worldwide. During 2017, around 18 million people died because of cardiac illnesses, representing the 31% of all deaths. Hypertension, defined as a chronic elevation of blood pressure, is the main risk factor for cardiovascular diseases and the main cause of atrial fibrillation. High blood pressure causes cardiac, renal, cerebral, and vascular damages, leading to early morbi-mortality. The global prevalence of high blood pressure is ca. 40% (Suárez Landazábal et al., 2019; Yusuf et al., 2020).

β−1 blocker drugs are one of the most used treatments of hypertension. Also, this drug family is widely prescribed for treating irregular heart rhythm as antiarrhythmic treatment (Ahad et al., 2015; Camm et al., 2010). Atenolol (AT) is a well-known, extensively-used β−1 blocker drug (Xue et al., 2015). It is classified as Class III drug in the Biopharmaceutics Classification System (BCS). This means that, orally administered, AT possesses high solubility but low permeability (Yang et al., 2007). In fact, it has been reported that AT has low paracellular diffusion and poor passive permeability, although it has recently been proposed that the OTC1 and PMAT transporters could also be involved

* Corresponding author at: Planta Piloto de Ingeniería Química (PLAPIQUI), CONICET-Universidad Nacional del Sur (UNS), Camino La Carrindanga km 7, 8000 Bahía, Blanca, Argentina.
E-mail address: nceschan@plapiqui.edu.ar (N.E. Ceschan).

https://doi.org/10.1016/j.ejps.2021.106108
Received 24 August 2021; Received in revised form 29 November 2021; Accepted 23 December 2021
Available online 26 December 2021

in its transport (Chen et al., 2017; Mimura et al., 2017). Also, it has been reported that AT has a short biological half-life and suffers an extensive hepatic first-pass metabolism (Lal and Datta, 2015; Mohanty and Subrahmanyam, 2017).

The oral recommended dose for AT tablets is between 25 and 100 mg, twice daily (Lal and Datta, 2015). Conventional oral administration usually results in erratic drug concentrations in plasma because of AT hydrophilicity, leading to reduction in the pharmacological effect or development of undesirable side effects. Ischemic colitis, nausea and diarrhea have been attributed to frequent oral administration and patients can also suffer central nervous system side effects (Gostick et al., 1977; Ramkanth et al., 2018).

To avoid these problems, different orally controlled-release formulations have been studied (Lal and Datta, 2015; Mohanty and Subrahmanyam, 2017; Mortazavi-Derazkola et al., 2017; Singh et al., 2006; Xue et al., 2015). Also, alternative noninvasive routes have been proposed. In particular, buccal patches (Hasnain et al., 2020) and transdermal delivery systems formulated as proniosomal gels or films containing AT have been developed (El-Assal, 2017; Gupta and Jain, 2004; Gupta and Jain, 2006; Kim and Shin, 2004; Mundargi et al., 2007; Ramkanth et al., 2018). In vitro characterization of these systems demonstrated enhanced AT penetration and controlled release. Sustained plasma concentrations were obtained for the transdermal formulations assayed in vivo (Gupta and Jain, 2004; Gupta and Jain, 2006; Ramkanth et al., 2018; Shin and Choi, 2003). Good pharmacokinetic control could be achieved with transdermal drug delivery systems or "patches" when formulations were optimized. Although findings in transdermal delivery are interesting, correct adhesion to the skin may be challenging, and transdermal systems are sometimes rejected by the patients due to esthetic aspects or discomfort (Kováčik et al., 2020; Tanner and Marks, 2008). Also, a mayor concern for transdermal delivery is related to the great variation in permeability through human skin (Todo, 2017)

The inhalatory administration is considered one of the main alternative noninvasive drug delivery routes and it is particularly interesting for cardiac targeting. This is because during absorption, drugs are predominantly first transported to the heart via the pulmonary vein (Miragoli et al., 2018). Considering this, inhalatory administration of AT could be an interesting alternative option in order to directly reach the cardiac tissue and decrease systemic exposure (Faragli et al., 2021; Rabinowitz and Zaffaroni, 2006). Pulmonary epithelium is relatively extensive and widely vascularized. In addition, there is little presence of efflux transporters, which favors drug absorption. Via this route, the onset of action can be relatively fast, metabolic enzymes levels are lower compared to hepatic ones, and drugs, even with different physicochemical properties, can be absorbed (Jain et al., 2020; Moebus et al., 2012; Pham et al., 2021; Videira et al., 2020). In particular, the pulmonary administration route presents competitive advantages as the alveolar membrane is extremely thin and possesses high permeability. Hence, the pulmonary absorption of different active pharmaceutical ingredients (APIs) is possible

The delivery of co-processed materials containing drugs and biodegradable polymers is an attractive option for inhalatory therapy that has been researched more in recent years. The combination of drugs with appropriate polymers allows: a) prolonging the drug residence time in the lungs (mucoadhesive polymers), which may enable the reduction of the daily dose and consequently minimizes adverse effects; b) facilitating mucus transport through lung lining fluid (mucopenetrating polymers); c) increasing stability during storage; d) avoiding particles recognition by alveolar macrophages, among other beneficial effects (Gallo et al., 2017; Ungaro et al., 2012b).

Ionic complexes containing AT and alginic acid (AA, an anionic polyelectrolyte) were previously described and obtained through co-processing by spray drying (Ceschan et al., 2016). The use of a relatively high atomization air flow rate and a high-performance cyclone allowed obtaining small size particles with suitable in vitro aerosolization performance when they were administrated by a dry powder inhaler (Ceschan et al., 2016). The aim of this work is to characterize the pharmaceutical and biopharmaceutical properties of atenolol-alginate microparticles administrated by nebulization as an alternative dosage form. The AA-AT system is proposed as a powdered product designed to be packed in individual containers, for further extemporaneous reconstitution in saline solution. To the best of our knowledge, the study of nebulized polyelectrolyte-drug systems has not been previously addressed, even though this type of aqueous formulations may present distinctive controlled-release properties (Olivera et al., 2017). To target the heart through lung administration, an adequate aerosolization and deposition performance, as well as suitable drug release and absorption patterns are needed. For this reason, the aerodynamic behavior of the formulation in the in vitro aerosolization test was evaluated by using a jet nebulizer. The mucoadhesive properties of the developed system, associated to the presence of AA in the formulation, and the ability of the ionic complex to reverse and release the drug to exert its therapeutic action were examined. Also, cell viability was evaluated after treating a cell line representative of alveolar epithelium with AT-containing formulations. Finally, the in vivo performance of the co-processed product was studied in an animal model, administering the material using the same jet nebulizer as that used in the in vitro aerosolization assay.

2. Materials and methods

Alginic Acid (molecular weight approximately 240 kDa) from Brown Algae (analytical grade, Sigma, Saint Louis, United States), atenolol and caffeine (pharmaceutical grade, Parafarm, Saporiti, Buenos Aires, Argentina), sodium chloride (analytical grade, Anedra, Buenos Aires, Argentina), potassium hydroxide (analytical grade, Cicarelli, Santa Fe, Argentina), F-12 K growth medium (ATCC, Manassas, United States), Dulbecco's phosphate buffered saline solution (Lonza, Walkersville, MD, United States), MTT reagent (Life Technologies, Oregon, United States), saline solution (pharmaceutical grade, Parafarm, Saporiti, Buenos Aires, Argentina), trifluoroacetic acid (TFA, Sigma Aldrich, St. Louis, United States), acetonitrile (AcCN, Baker, Madrid, Spain) and bidistilled water were used.

2.1. Methods

2.1.1. Liquid formulations and characterization

Alginic acid (AA) is insoluble but dispersible in water (Ceschan et al., 2014), while atenolol (AT) is a water soluble drug (Demou et al., 1994). AA was dispersed in distilled water and atenolol (as a powder) was incorporated under magnetic stirring (see AA-AT formulation in Table 1), obtaining a stable dispersion (Ceschan et al., 2014). When both materials are mixed in water, ionic interactions between ionizable groups occur. The drug/polyelectrolyte ratio was fixed in order to obtain a 75% neutralization of the available acidic groups of AA (4.55×10^{-3} equivalents per AA gram (Ceschan et al., 2014)). Distilled water was used to make 200 mL of dispersion, being the pH value around 4.15 (determined by using a pHmeter Orion 410A Cole Parmer, Vermon Hills, United States). When a formulation with this pH value reaches the lungs, it causes severe cough, bronchospasm and inflammatory reactions (Surber et al., 2010). For this reason, the pH of the dispersion was adjusted close to 7 by adding KOH (0.09567 N). Dispersions were

Table 1
Liquid formulations composition.

Sample	AT (g)	AA (g)	KOH (g)	Total solid content (W/V%)	Relative composition(g_{AT}/g_{solid})
AT	3.21	–	–	1.6	–
AA-AT	1.52	1.68	0.11	1.7	0.46

prepared by triplicate. Also, 200 mL of a water solution containing pure AT was also prepared.

Particle size distribution of the dispersions was measured by laser diffraction (LA 950V2, Horiba, Kyoto, Japan), using the wet method by filling the measurement cell with saline solution. The dispersion size distribution was studied immediately after preparation, after 15 min and one day from the suspension preparation. Size is reported as median diameter (D_{50}) and distribution width is informed as *span*. The *Span* index was calculated as follows:

$$Span = \frac{D_{90} - D_{10}}{D_{50}} \quad (1)$$

where D_{90}, D_{50} and D_{10} are the diameters where the 90%, 50% and 10% of the population lies below each value, respectively. A distribution can be considered relatively narrow if the *span* value is less than 2 (Palazzo et al., 2013). The experiments were performed in triplicate.

2.1.2. Spray drying (SD) and powder characterization

Dispersions obtained in Section 2.2.1 were atomized under constant magnetic stirring in a negative pressure laboratory scale SD equipment (Mini Spray Dryer B-290, BÜCHI, Flawil, Switzerland). A two-fluid nozzle with a cap-orifice diameter of 0.5 mm was used. Operating conditions were selected accordingly to a previous work (Ceschan et al., 2016): air inlet temperature (co-current): 140 °C, liquid feed flowrate: 6 mL/min, atomization air flowrate: 742 L/h and drying air flowrate: 35 m^3/h. A high-performance cyclone was used to collect the dried powders. The obtained material was weighed, packed in sealed amber bottles and stored in a desiccator for further characterization. The process yield was calculated as the ratio of the weight of product collected after the SD process respect to the total solid content fed to the dryer.

The particle size distribution of the powder was measured by laser diffraction by using the wet and also the dry powder method. For the former, microparticles were dispersed in saline solution and size was determined at different times. For the size analysis using the dry method, the SD powders were dispersed in lactose to improve the sample flow from the feed hopper to the measuring cell as explained elsewhere (Ceschan et al., 2014). Size is reported as D_{50} and distribution width is informed as *span*.

Moisture content of the powders was determined immediately after the spray drying process in a halogen moisture analyzer (MB45, Ohaus, Pine Brook, United States). About 500 mg of SD product was heated up to 105 °C until the weight change was less than 1 mg in sixty seconds.

AT mass concentration in the obtained products was determined by UV-spectrophotometry (T60, PG instruments, Lutterworth, UK) at 274.6 nm by dissolving the powders in distilled water.

Glass transition temperature (T_g) was studied by differential scanning calorimetry (DSC). Thermograms were obtained (Pyris 1, Perkin Elmer, Massachussets, United States) from 5 mg of AA-AT placed in closed aluminum pans under nitrogen atmosphere flowing at 40 mL/min. Sample was heated from 30 to 180 °C at 10 °C/min, then cooled down to 30 °C and finally temperature was raised up to 180 °C (at 10 °C/min). T_g was estimated by using the half ΔCp method (Gallo et al., 2011).

2.1.3. Aerodynamic behavior

The aerodynamic behavior of different materials was assayed using a Next Generation Pharmaceutical Impactor (NGI, Copley Scientific, Nottingham, UK) following the ⟨1601⟩ USP chapter (USP38-NF33, 2015). The NGI equipment is composed by seven stages (S1-S7), a micro-orifice collector (MOC), an induction port (IP) and a vacuum pump that allows simulating the inspiration. A jet nebulizer (NA182 plus, ASPEN, Buenos Aires, Argentina) was connected to the IP by using a silicone adaptor. An external filter was placed between the NGI equipment and the vacuum pump. All NGI components were refrigerated during 90 min prior the tests to avoid both droplet growth and evaporation, improving the accuracy of the measured aerodynamic size distribution (Berg et al., 2007).

Different AT doses were assayed in the NGI equipment. The co-processed powders (50 or 100 mg) were suspended in 4 mL of saline solution and placed in the nebulizer cup. For comparative purposes, 25 or 50 mg of AT in 4 mL of saline solution were also nebulized in the NGI equipment. The NGI vacuum pump flowrate was fixed at 15 L/min and the assay was continued for 15 min. The drug deposited on the NGI system and the remaining in the nebulizer cup were recovered with an adequate amount of distilled water. AT concentration in each NGI component was quantified by UV spectrophotometry at 274.6 nm. The assay was performed by triplicate. Mass balance closure was evaluated for all the aerosolization experiments. Only those experiments where the drug mass recovery was between 85 and 115% were used to stablish the aerodynamic product performance.

The NGI characteristic parameters: Mass Median Aerodynamic Diameter (MMAD) and Geometric Standard Deviation (GSD) were calculated following the ⟨1601⟩ USP chapter (USP38-NF33, 2015).

The MMAD is defined as the diameter at which 50% of the drug is collected in larger particles and the remaining 50% is collected in smaller particles and was calculated from a drug mass cumulative distribution (built considering the drug mass collected in NGI-1 to 7 stages, MOC and external filter).

The Geometric Standard Deviation (GSD), that represents the spread of an aerodynamic particle size distribution, was calculated as follows:

$$GSD = \left(\sqrt{D_{84}/D_{16}}\right) \quad (2)$$

where D_{84} and D_{16} represent the diameters at which 84% and 16% of the drug mass is recovered from the NGI 1 to 7 stages, MOC and external filter, respectively. Aerodynamic size distribution is considered narrow if GSD is lower than 3 (Razavi Rohani et al., 2014).

Also, the Fine Particle Fraction (FPF) was calculated. This fraction is defined as the percentage of cumulative drug mass with aerodynamic diameters lower than 5 or 3 μm respects to the total drug mass recovered from the IP, NGI 1–7 stages, MOC and external filter (Ceschan et al., 2016). In general terms, aerosols should have aerodynamic diameters less than 5 μm to enter the lungs. However, for systemic treatments, aerodynamic diameters lower than 3 μm are needed to ensure aerosol targeting to the alveolar membrane (Newman and Chan, 2008).

2.1.4. Drug release experiment

In order to study the capability to release the drug from the AA-AT polyelectrolyte complex, vertical Franz Cells operated at 37 °C were used. Receptor and donor compartments were limited by a dialysis cellulose membrane (Sigma, molecular weight cut-off: 14,000 Da). The receptor compartment (60 mL) was completed with degasified saline solution and was kept under constant magnetic stirring.

For the assay, necessary amounts of the SD powders (either containing AA-AT or pure AT) were dispersed in saline solution to achieve an AT concentration of 5 mg/mL. A volume of 5 mL of these dispersions was placed in the donor compartment. This represents the lower amount of co-processed materials and pure AT that was assayed in the NGI equipment. Samples of 2 mL were withdrawn from the receptor compartment at 5, 15, 30, 60, 90, 120, 180, 240, 300 and 360 min and replaced with fresh medium. Atenolol content in the samples was assayed by UV spectrophotometry at 274.6 nm. The atenolol release profiles were compared by using the similarity factor f_2, defined as follows (Ong et al., 2011):

$$f_2 = 50\log\left\{\left[1 + \left(\frac{1}{n}\right)\sum_{t=1}^{n}(R_t - P_t)^2\right]^{-0.5}\right\}100 \quad (3)$$

where n represents the number of experimental points and R_t and T_t are the drug release percentage at time t from the reference (pure AT sample) and the complex carrying the drug (AA-AT sample), respectively.

Formulations are considered similar if the f_2 value is higher than 50 (Ong et al., 2011). The experiments were performed in sextuplicate.

2.1.5. Mucoadhesion assay: tensile strength

The mucoadhesion properties of the reconstituted SD materials were studied using a TA Plus texture analyzer (Lloyd Instruments, Godalming, UK) equipped with a 5-kg_f load cell. The technique was adapted from Ivarsson and Wahlgren (Ivarsson and Wahlgren, 2012). Briefly, 0.1 mL of a mucin solution (3% in buffer phosphate pH 7.4 kept at 37 ± 0.5 °C) was placed on a filter paper (diameter: 2 cm). The filter paper was attached to a stationary surface and the mucin solution was allowed to stand for 15 min.

The SD powders (either containing AA-AT or pure AT) were dispersed in saline solution to achieve AT concentration of ca. 5 mg/mL. A filter paper (diameter: 1 cm) was imbibed in the dispersion and attached to the movable probe, placed above the stationary surface. Then, the movable probe was lowered, without applying any force, until it soaked in the mucin solution for 3 min. Finally, the probe was raised at withdrawal speed of 0.1 mm/s. The maximum detachment force (MDF) and the total detachment work (TDW) were measured using the texture analyzer software (Nexygen Plus). Results reported are given as average of ten measurements.

2.1.6. Cytotoxicity assay

In order to analyze the potential cytotoxic effects of the developed materials in representative pulmonary cell lines, the MTT [3-(4,5-dimethylthiazol-2-yl)−2,5-diphenyltetrazolium bromide] colorimetric assay was performed in A-549 (ATCC® CCL-185®) cells. This test provides a quantitative measurement of the cell viability. The reduction of the MTT to formazan occurs only in the mitochondria of viable cells. This cell line has been widely used to investigate the effect of drug administration to the lungs (Forbes and Ehrhardt, 2005) and was selected for being representative of alveolar epithelium as the developed particles are intended to systemic administration of atenolol.

A-549 cells were plated in a 96-well plate at 5000 cells/well and cultured at 37 °C in 5% CO_2 for 24 h. After that time, 100 μL of redispersed powder in growth medium containing 0.25, 0.5, 1.0 and 2.0 mg/mL of the complex AA-AT was added to the wells. The 0.5 and 1 mg/mL concentrations were selected considering the microparticles composition, the liquid lung volume (50–100 mL) (Yeh and Schum, 1980) and the maximum recommended AT dose for inhalatory route (20 mg) (Rabinowitz and Zaffaroni, 2006). Cells without treatment were cultured and considered the positive control. Plates were incubated for 24 h. After that time, the MTT solution was added. Two hours later, the formed formazan was quantified by adding DMSO and measuring the UV-absorbance of each cell well at 540 nm in a multimode microplate reader (Infinite® 200 PRO, Tecan Systems, USA). Treatments were applied by sextuplicate. Cell viability is calculated as follows:

$$Cell\ viability = \left(\frac{Treatment\ absorbance}{Control\ absorbance}\right)100 \quad (4)$$

2.1.7. In vivo microparticles nebulization

Swiss mice (provided by the Facultad de Veterinaria, UNLP, Argentina), weighting between 18 and 20 g, were used as experimental animals. Polymeric microparticles carrying AT were pulmonary administrated by using a jet nebulizer (NA182 plus, ASPEN, Buenos Aires, Argentina). In order to accurately determine AT concentration in biological samples, around 100 mg of the polyelectrolyte complex (the highest one assayed in the NGI equipment) was weighted, dispersed in 4 mL saline solution and placed into the nebulizer cup. Mice were nebulized using a custom whole-body inhalation chamber during 20 min. A description of this exposure chamber can be found elsewhere (Islan et al., 2017).

Mice were divided into four groups of $N = 3$. Intracardiac blood samples were obtained from each mouse at predetermined times (t): 0, 20, 60, 100, and 140 min, where $t = 0$ represents the condition before the nebulization and t = 20–140 represent the time elapsed from nebulization beginning. Then, animals were euthanized and lungs were removed, weighted and frozen. Blood plasma was obtained by centrifugation of the samples, measured the volume and also frozen.

All experiments were performed according to protocol #002–17–16 approved by the Ethical Committee of the Facultad de Ciencias Exactas de la UNLP (Argentina).

2.1.8. AT quantification of biological samples

Drug quantification was performed using an UHPLC equipment (Dionex Ultimate 3000 Thermo Scientific, USA) coupled to a UV-diode array detector (DAD-3000). The stationary phase was a C-18 column (150 × 4.6 mm, 5 μm, Phenomenex, USA). The mobile phase was a mixture of 20 mM phosphate buffer pH 2.45/MeOH (85/15). An isocratic 1.2 mL/min flowrate was used and the detection wavelength was set at 225 nm.

Plasma and lung samples were prepared as follows. For plasma analysis, 5 μL of Caffeine (CA) stock solution (internal standard, ca. 500 mg/L) were added to 100 μL of sample. After a few minutes at room temperature, a mixture of 10% TFA:AcCN (70:30) was carefully added and then the sample was cooled down using an ice bath for protein precipitation. The sample was refrigerated during 15 min and centrifuged 20 min at 4000 rpm. The supernatant was separated, centrifuged 10 min at 12,000 rpm and injected in the UHPLC by duplicate. The lungs (previously weighed) were placed in 2 mL of bicarbonate buffer (0.2114 g of $NaHCO_3$ in 100 mL of water, pH 9.6) and 100 μL of CA stock solution were added. The homogenized mixture was sonicated 30 min in an ice bath and then centrifuged at 3500 rpm during 30 min. The supernatant obtained from each sample was divided into two aliquots of around 800 μL, which were transferred to conical base tubes. A 10% TFA:AcCN (70:30) mixture was added to each tube for protein precipitation. The sample was refrigerated during 15 min and centrifuged 20 min at 4000 rpm. The supernatant was separated, centrifuged 10 min at 12,000 rpm and injected in the UHPLC. Drug-free plasma and lung samples were treated in the same way as previously described. In these cases, along with the internal standard, 5 μL (for plasma standard) or 50 μL (for lung standard) of AT stock solution (approximately 1000 mg/L) were added.

2.1.9. Statistical analysis

The significant differences between mucoadhesion properties, cell viability, and in vitro aerosolization behavior were determined by means of one-way ANOVA, followed by the Least Significant Difference (LSD) *post hoc* multiple comparison method. Statistical significance was established through the *p*-value: values lower than 0.05 were considered statistically significant. Before the analysis, homoscedasticity and normality ANOVA's assumptions were checked by the Levene test and Standard Kurtosis values, respectively (Nimon, 2012; Villanueva et al., 2000).

3. Results

3.1. Raw material and dispersions characterization

As above mentioned, Table 1 shows the composition of the formulations that were processed by SD. For AA-AT sample, after the KOH addition, the pH was 6.53 ± 0.04. Characteristic parameters of the particle size distribution of the liquid dispersion AA-AT are shown in Table 2 after different times from dispersion preparation. As can be seen, D_{50} value was higher than 68 μm for all the tested times. This value is markedly bigger than the ones needed for inhalatory administration (0.5–5 μm) (Traini, 2013; Verma et al., 2015). For this reason, dispersions were processed by spray drying in order to obtain microparticles with adequate attributes for the proposed application. In this way, a powder to be reconstituted before nebulization was developed. Additionally, the dried powders possess some competitive advantages in

Table 2
D_{50} and span values for the feed and products of the spray drying process.

Sample	State of sample	Laser diffraction method	t	D_{50} ± SD [μm]	Span ± SD [−]
AA-AT liquid formulation	Liquid	Wet	0	68.20±3.69	1.53±0.23
			15 min	69.33±7.91	1.49±0.25
			24 h	73.48±3.90	2.10±0.06
AA-AT co-processed	Resuspended powder	Wet	0	2.56±0.04	1.63±0.04
			15 min	2.82±0.01	1.19±0.01
			24 h	2.77±0.05	1.51±0.01
	Powder	Dry	–	3.57±0.21	0.88±0.08
AT	Powder	Dry	–	5.35±0.43	2.15±0.25

SD: standard deviation; t: time.

terms of physical and microbiological stability over liquid formulations (Ivanovska et al., 2014).

3.2. Spray drying process and microparticles characterization

The liquid formulations of Table 1 were processed in a spray dryer using the process parameters detailed in Section 2.2.2.

Table 3 shows the process yield (Y), the outlet air temperature (T_{out}), the powder moisture content (MC) and relative composition of the powder. The T_{out} was lower than 65 °C for both, pure AT and the AA-AT, products. This value is lower than the reported degradation temperatures for AT (around 200 °C (Wesolowski and Rojek, 2013)) and AA (around 190 °C (Soares et al., 2004)). Thus, no thermal degradation of AT or AA should be expected. Also, T_g value for the AA-AT material was 94.65 °C. This relatively high T_g value would avoid stability problems during handling and storage.

The process yield was 85% for the AA-AT product, a very high value for a lab-scale SD equipment. This value is around 15% higher than the one obtained for the pure AT. The moisture content for pure AT and the co-processed product were 0.63 and 4.90%, respectively. These values are in good agreement with the different hygroscopicity nature of the materials (Ceschan et al., 2014; Rowe et al., 2009). Moisture values lower than 5% have been reported as suitable for long-term storage (Tontul and Topuz, 2017).

The mean relative composition of the powder was 0.43 g_{AT}/g_{solid}, this value is very close to the liquid formulation composition (see Table 1). This concordance between the values indicates that the dispersion was stable during SD process and no differential losses occurred.

Finally, for the powders AA-AT and pure AT, the median diameters (D_{50}) and the *span* values are shown in Table 2. The D_{50} value obtained by using the dry method was 3.57 μm for the AA-AT product. This small particle size is a desired attribute for inhalatory administration. The pure AT D_{50} value was higher than the one obtained for the co-processed material. The *span* value, lower than 2 for the microparticles AA-AT, indicated that the particle size distribution was narrow (Palazzo et al., 2013). In order to assess the ionic complex size distribution in saline solution, AA-AT microparticles were resuspended in this medium and D_{50} was determined by using the wet method. As can be seen in Table 2, the D_{50} for the co-processed product was lower than 3 μm, adequate value for inhalatory administration. Also, D_{50} result was similar for 0 and 15 min and even one day after the resuspension, indicating that microparticle geometric size did not change over time. For all the tested times, the distributions were narrow (*i.e. span* values lower than 2).

Table 3
Process yield (Y), air outlet temperature, moisture content (MC) and relative composition of the SD products.

Sample	Y (%)	T_{out} (°C)	MC (%)	Relative composition(g_{AT}/g_{solid})
AT	73.29±3.38	64.3 ± 1.53	0.63±0.08	–
AA-AT	85.25±1.68	63.3 ± 0.58	4.90±0.42	0.43±0.02

3.3. Aerodynamic performance

Among different inhalatory administration systems, nebulized formulations are useful for assessing new pulmonary products without the need of a device development (Traini and Young, 2009). According to the USP ⟨1601⟩ chapter, MMAD and GSD values are the parameters needed to characterize nebulized systems (USP38-NF33, 2015). In this work, fine particle fractions (FPF) for representative diameters were also calculated.

Table 4 shows the MMDA, GSD and FPF values for the AT and the AA-AT reconstituted powders. The MMAD was 3.41 and 3.61 μm for the AA-AT and AT powders (when AT dose was 25 mg), respectively. MMAD was slightly bigger when powders carried 50 mg of AT (3.60 and 3.72 for AA-AT and AT, respectively) were analyzed. The GSD values were lower than 3 for both samples and concentrations assayed (*i.e.* aerodynamic particle distributions were narrow (Razavi Rohani et al., 2014)). For jet nebulizers and different products (commercial and in development formulations), the MMAD values were found in the 3.38–7.08 μm range (Amani et al., 2009; Beng et al., 2018; Kamali et al., 2016; Poli et al., 2007). The nebulized reconstituted powders provide MMADs within the reported range, and they are particularly small which is a desired property for systemic treatments.

Besides MMAD and GSD values, two fine particle fractions were calculated, FPF < 5 μm and FPF < 3 μm, to assess the capability of the powders to reach the lung and the alveolar membrane, respectively (see Table 4). These fractions allow stablishing, to some extent, *in vitro-in vivo* correlations (Mitchell et al., 2007). In this work, the FPF < 5 μm value is between 62 and 66% for pure AT and 65–68% for AA-AT. The differences between both FPFs were not statistically significant neither between samples nor between concentrations assayed (p-value > 0.05). These values are relatively high compared to the ones found in literature for formulations assayed using jet nebulizers (19–62% (Amani et al., 2009; Amani et al., 2010; Beng et al., 2018; Carrigy et al., 2017; Jaafar-Maalej et al., 2010; Johnson et al., 2008)). FPF < 3 μm of AA-AT system was around 40%, while for pure AT ca. 37%. The values obtained for this fraction are close to the one reported by Johnson et al. In fact, these authors obtained a FPF value of 40.7% for particles with aerodynamic diameters lower than 3.3 μm when assayed an inhaled recombinant human DNase I using a jet nebulizer (Johnson et al., 2008). Thus, in this work, it is predicted that about 40% of the emitted fraction

Table 4
Aerodynamic performance of AA-AT and pure AT samples.

Sample	AA-AT	AT	AA-AT	AT
Mass resuspended (mg)	50	25	100	50
AT recovery (%)	95.34±6.07	95.37±6.65	94.75±5.26	99.34±3.30
FPF < 5 μm (%)	68.38±3.73	66.45±1.07	65.42±1.63	62.04±3.92
FPF < 3 μm (%)	41.89±2.22	38.46±1.15	37.21±2.81	36.99±2.77
MMAD (μm)	3.41±0.09	3.61±0.12	3.60±0.13	3.72±0.21
GSD	2.14±0.03	2.05±0.03	1.86±0.11	1.96±0.17

would reach the alveolar membrane and be absorbed for systemic action.

The aerodynamic performance of the aerosol indicates that the nebulization of the reconstituted AA-AT powder is a promising alternative for administering AT to the heart by using the inhalatory route, even at different AT doses.

In a previous work, a similar AA-AT particulate system was developed for inhalatory administration as dry powder inhaler (DPI) (Ceschan et al., 2016). Although this formulation had in vitro adequate aerodynamic performance for the proposed application, the nebulization of the AA-AT resuspension also showed satisfactory aerosolization behavior. In fact, FPF < 3 μm value was 37% for the AA-AT powder when 100 mg material was loaded in the nebulizer cup and 29% for a dry powder inhaler formulation carrying 25 mg of AA-AT (Ceschan et al., 2016). This result would extend the application of the formulation for patients with limited pulmonary capacity (Mahler et al., 2019; Taffet et al., 2014).

3.4. In vitro drug release

In the Franz cells experiment, the presence of AT in the receptor compartment indicates that the drug was able to dissociate from the polyelectrolyte, while the alginic acid is retained in the cellulose membrane. This dissociation occurs due to an ionic exchange process with the ions (Na and Cl) of the saline solution as it was previously demonstrated for swellable atenolol-alginic acid matrices (Ramırez Rigo et al., 2006).

Fig. 1 shows the atenolol release profiles for the reconstituted AA-AT and AT powders. These two profiles can be considered similar as the similarity factor f_2 was 68 (profiles can be considered similar if the f_2 value is higher than 50 (Ong et al., 2011)). The observed behavior suggested that the co-processed material in simulated physiological media has the capability to release the active ingredient by ionic exchange (Ramırez Rigo et al., 2006) and the released drug passed through the membrane. Thus, the polymer addition to the particle formulation would not adversely affect the drug availability in the lung membrane.

3.5. In vitro mucoadhesion test

The mucoadhesion of the AA-AT product was studied and compared with pure AT. This test was carried out since mucoadhesive materials can modulate the residence time of the drug in the lung modifying active ingredient clearance (Dong et al., 2020; Khutoryanskiy, 2011; Ungaro et al., 2012a).

Table 5 shows the maximum detachment force (MDF) and the total work of adhesion (TWA) required to detach the probe from the AA-AT and pure AT reconstituted powders. The test carried out with mucin solution and without the active ingredient, corresponds to the control test (minimum force required for the probe detachment). When the assay was performed with reconstituted pure AT, the MDF and TWA values were similar to the ones obtained using only mucin. In fact, the mean values of these two materials were not statistically different (p-value > 0.05), indicating that AT does not strongly interact with mucin. On the other hand, the ionic complex required a greater strength to detach the probe, in concordance with the mucoadhesive properties described for AA (Séchoy et al., 2000). The MDF and the TWA differences between AA-AT and AT were statistically significant (p-value < 0.05), indicating that the AA-AT material enhances the mucoadhesive properties.

For anionic polymers, interaction with mucine chains has been explained by ionic interaction at lower pH values. When medium pH increases, mucin chains are negatively charged and repulsion between both negatively charged chains is expected although adhesion still occurs (Khutoryanskiy, 2011). In addition, other authors demonstrated that alginic acid can permeate through intestinal mucus pores (Mackie

Table 5
Maximum detachment force (MDF) and total work of adhesion (TWA).

Material	MDF(N)	TAW(J, x10^{-4})
AT	0.53±0.09	6.35±1.67
AA-AT	1.03±0.22	17.81±3.63
Mucin	0.51±0.04	6.25±2.43

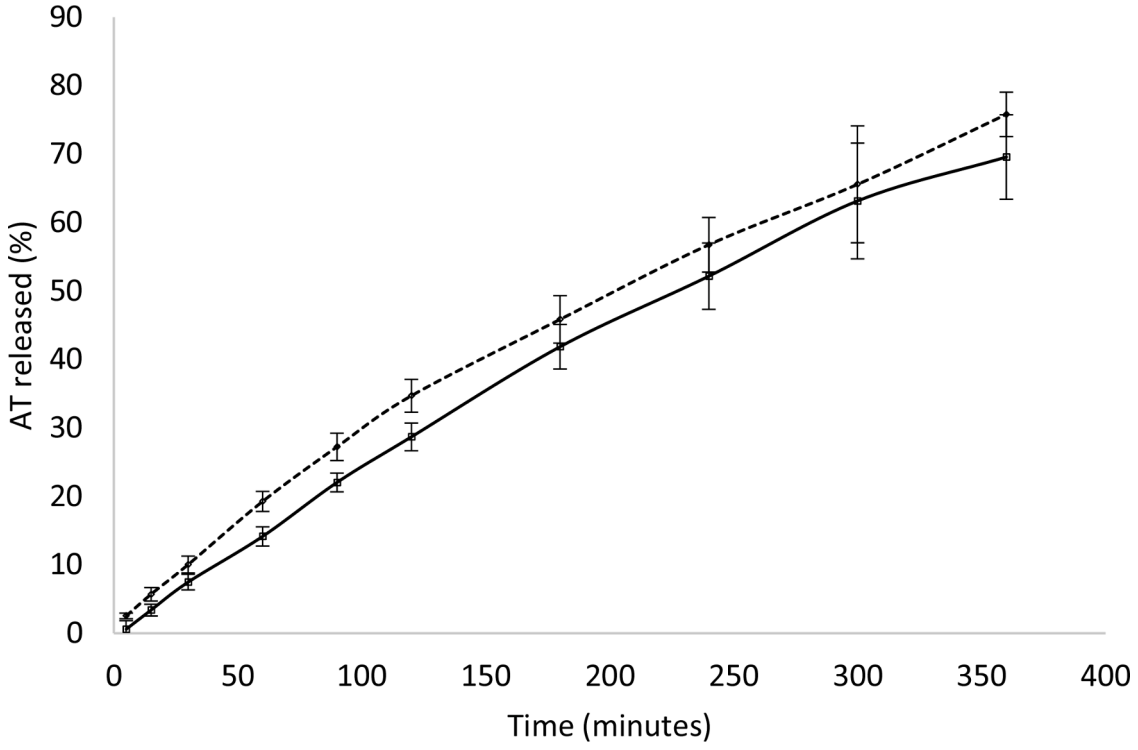

Fig. 1. AT release from resuspended powders of AT (dashed line) and AA-AT (continuous line).

et al., 2016). Further studies are necessary to fully understand the interaction between mucin and the developed material. The influence of AA in lung retention is discussed below.

3.6. Cytotoxicity assay

In order to assess the cytotoxicity of the new material in a cell line representative of alveolar epithelium, Fig. 2 shows cell viability for the AA-AT sample. As it can be seen, for all the tested AA-AT concentrations, the cell viability was similar to the control condition. In fact, the observed differences were not statistically significant for all the treatments (p-value > 0.05). It is important to highlight that the maximum concentration assayed corresponds to a drug dose in the lung equivalent to 100 mg (considering a pulmonary volume of 100 mL). In this way, this dose is 5 times higher than the maximum one for the hypertension treatment by the inhalatory route (Rabinowitz and Zaffaroni, 2006). Even though these results are promising, toxicity studies of higher doses of AT and/or AA in the lung have not yet been addressed.

From the previous assays, it can be concluded that the presence of AA in the SD products confers mucoadhesive properties to the ionic complex, being not affected the release of the drug from the dissolved material and its transport through the cellulose membrane. Also, the developed material did not affect cell viability or the aerodynamic performance.

3.7. Preliminary pharmacokinetic study

The AA-AT ionic complex was administered to mice by a nebulization system in order to study the in vivo performance of the developed formulation. For comparative purposes, pure AT was also studied in the mice model.

Fig. 3 shows pulmonary AT concentration (expressed as μg of drug per g of tissue) for both, the AA-AT system and the pure AT. As can be seen in these profiles, almost 6.5 μg/g of AT was deposited in the lungs right after the nebulization ending ($t = 20$) for AA-AT and AT. This similar value suggests that the AT contained in the ionic complex is able to reach comparable lung interstices. However, for $t = 60$, a higher AT lung concentration was detected for AA-AT than for AT. This could be related to the mucoadhesive properties of the polymer (Mackie et al., 2016; Nordgård et al., 2014). By inspection of Fig. 3, the maximum AT concentration in lung (lung C_{max}) and the time at which this concentration is reached (lung t_{max}) were estimated for both treatments applied. As can be seen, experimental lung C_{max} and t_{max} were 6.82 μg/mL and 20 min for AT, respectively, and 7.52 μg/mL and 60 min for AA-AT. Also, the area under the curve from the AT lung concentration vs time data ($AUC_{0–140}$) was calculated. This value was 616.29 μg min/mg for the pure drug and 682.48 μg min/mg for the AT carried in the AA-AT ionic complex. Although further studies are necessary, the preliminary results presented in this work would indicate that the developed formulation increases lung residence time in the lungs during the first hour after administration.

Also, the AT concentration in plasma was studied (expressed as μg of AT in one mL of plasma). Results are shown in Fig. 4. The lowest level of AT in plasma was detected immediately after the nebulization ended. By inspection of Fig. 4, the maximum AT concentration in plasma (plasma C_{max}) and the time at which this concentration is reached (plasma t_{max}) were estimated for both, the pure drug and the AT carried in the microparticles. As can be seen, experimental plasma C_{max} was 2.2 and 2.8 μg/mL for AT and AA-AT, respectively, while t_{max} was 100 min for both conditions assayed. This is in good agreement with the similar profiles observed for AA-AT and pure AT in the Franz cells experiment. Although these pharmacokinetic parameters were similar for the pure AT and the drug carried in the AA-AT system, the $AUC_{0–140}$ was somehow different. In fact, the $AUC_{0\text{-}140}$ for the pure drug was 182.8 μg min/mL and 275.7 μg min/mL for the AT in the AA-AT system.

The higher plasma AUC for the drug carried in the ionic complex suggests an increase in the AT bioavailability when administered in this system, a behavior already described for several other drugs and administration routes (Hariyadi and Islam, 2020; Radwan et al., 2017). This, in turn, may be due to the combination of two effects: an increased residence in lungs and an increased absorption through lungs epithelium due to the presence of the mucopenetrating polymer. In fact, polymeric virus mimicking particles (described as mucopenetrating) with positive and negative charges have the capability to interact between them and not with mucine chains enhancing drug permeation (Netsomboon and Bernkop-Schnürch, 2016). In this work, negative groups of AA were neutralized with atenolol positive charges and KOH (Olivera et al., 2017). Although more experiments are needed to fully address this

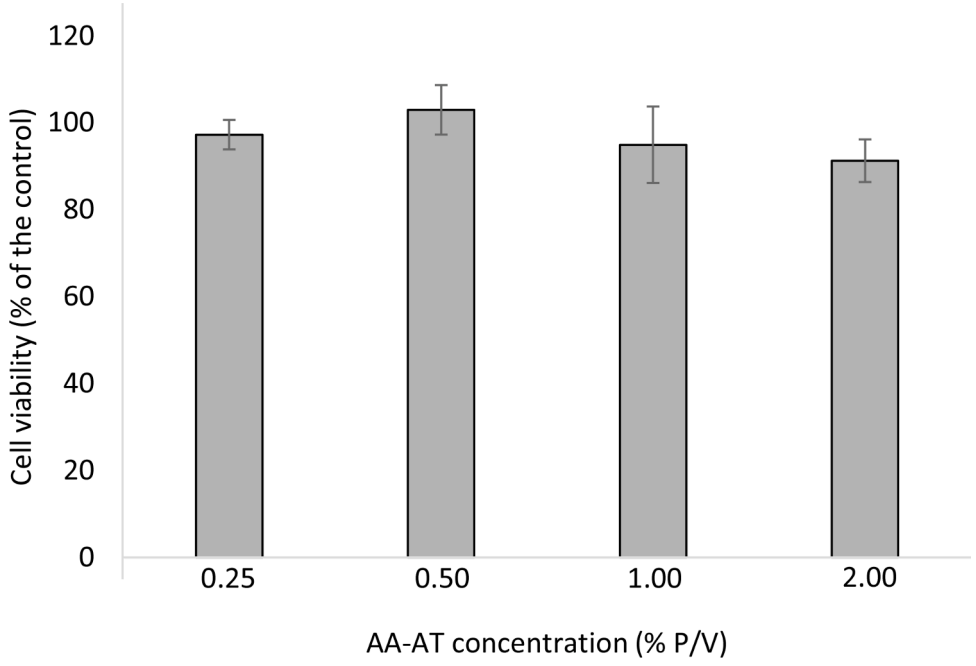

Fig. 2. Cell viability, expressed as% of the control, for different AA-AT concentrations: 0.25, 0.50, 1.00 and 2.00%.

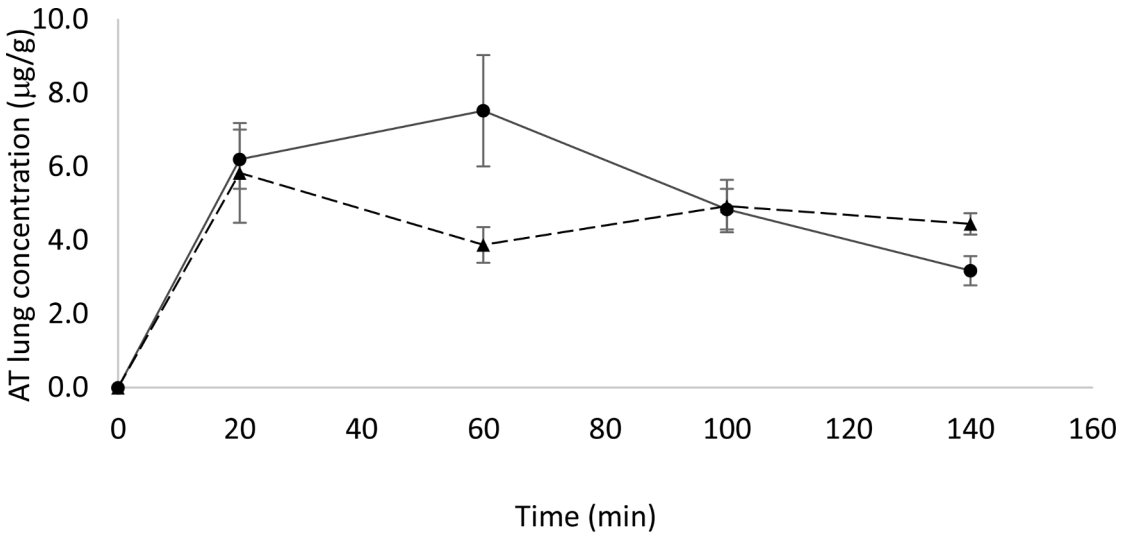

Fig. 3. AT lung concentration at different sampling times after AT (dashed line) and AA-AT (continuous line) nebulization.

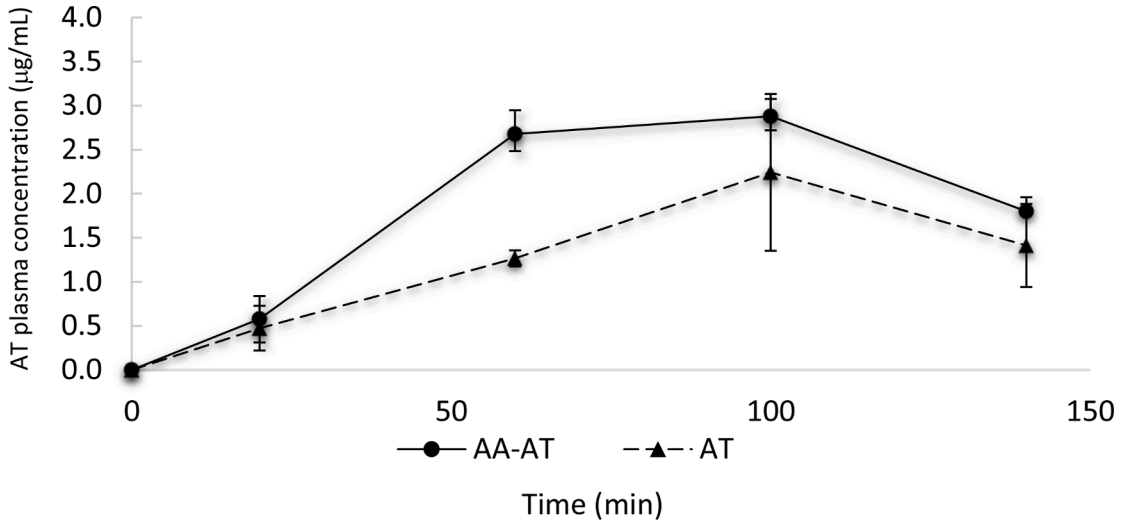

Fig. 4. AT plasma concentration at different sampling times after AT (dashed line) and AA-AT (continuous line) nebulization.

hypothesis, it is believed that the mucopenetrating effect is the predominant one, since the 50% increase in systemic bioavailability achieved by the microparticles (as measured from plasma AUC) is higher than that can be expected from the ca. 10% increase in lung AUC values.

4. Conclusions

In this work, pharmaceutical and biopharmaceutical properties of reconstituted AA-AT microparticles administrated by nebulization were studied. This particulate system was prepared by spray drying in order to obtain a stable product with adequate geometric and aerodynamic diameters for treating hypertension and arrhythmia by inhalatory administration.

Aerodynamic performance demonstrated that the nebulization of the inhalatory developed system has the capability to reach the lung. In fact, more than the 65% of the nebulized formulation possessed a fine particle fraction lower than 5 μm. What is more, FPF for particles with aerodynamic diameters smaller than 3 μm was around 40%, indicating that this amount of AT has the capability to be deposited and absorbed in the alveolar membrane.

Experiments in Franz cells demonstrated that the ionic complex releases the drug by ionic exchange and that the released drug permeated through the cellulose membrane. Around the 70% of the AT located in the donor compartment at the beginning of the experiment was quantified in the receiving one after 6 h.

The ionic complex also proved to be mucoadhesive and did not affect A-549 cell viability, even for a concentration 5 times higher than the maximum recommended AT dose for treating hypertension by pulmonary route.

Finally, the preliminary pharmacokinetic assay demonstrated that the formulation was able to reach the lungs and deposit at the alveolar membrane, effectively delivering AT through this membrane to the systemic circulation. This result highlights the potential of the developed system for cardiac drugs delivery through the lungs. Future comparison between different administration routes will be also addressed in order to confirm the auspicious results here presented.

CRediT authorship contribution statement

Nazareth E. Ceschan: Investigation, Methodology, Validation, Formal analysis, Writing – original draft, Visualization. **Sebastián Scioli-Montoto:** Investigation, Validation, Methodology, Formal analysis. **María Laura Sbaraglini:** Investigation, Methodology, Formal analysis, Resources. **María Esperanza Ruiz:** Methodology, Formal

analysis, Writing – review & editing, Resources. **Hugh D.C. Smyth:** Methodology, Writing – review & editing, Resources. **Verónica Bucalá:** Writing – review & editing, Resources, Project administration, Funding acquisition. **María V. Ramírez-Rigo:** Conceptualization, Supervision, Writing – review & editing, Resources, Project administration, Funding acquisition.

Acknowledgments

This work was funded by CONICET (PIP 11220150100704CO), UNS (PGI 24/B252), FONCYT (PICT-2016–0976; PICT-2018–00735, PICT-2016–11), UNLP (11/X878) and UNLP Young Scholars Grant. The authors thank F. Cabrera (PLAPIQUI), L. Leidi and LIDeB staff for their technical assistance.

References

Ahad, A., Al-Jenoobi, F.I., Al-Mohizea, A.M., Akhtar, N., Raish, M., Aqil, M., 2015. Systemic delivery of β-blockers via transdermal route for hypertension. Saudi Pharm. J. 23, 587–602. https://doi.org/10.1016/j.jsps.2013.12.019.

Amani, A., Chrystyn, H., Clark, B.J., Abdelrahim, M.E., York, P., 2009. Evaluation of supercritical fluid engineered budesonide powder for respiratory delivery using nebulisers. J. Pharm. Pharmacol. 61, 1625–1630. https://doi.org/10.1211/jpp/61.12.0006.

Amani, A., York, P., Chrystyn, H., Clark, B.J., 2010. Evaluation of a nanoemulsion-based formulation for respiratory delivery of budesonide by nebulizers. AAPS Pharm. Sci. Tech. 11, 1147–1151. https://doi.org/10.1208/s12249-010-9486-9.

Beng, H., Zhang, H., Jayachandra, R., Li, J., Wu, J., Tan, W., 2018. Enantioselective resolution of Rac-terbutaline and evaluation of optically pure R-terbutaline hydrochloride as an efficient anti-asthmatic drug. Chirality 30, 759–768. https://doi.org/10.1002/chir.22846.

Berg, E., Svensson, J.O., Asking, L., 2007. Determination of nebulizer droplet size distribution: a method based on impactor refrigeration. J. Aerosol Med. Depos. Clear. Eff. Lung 20, 97–104. https://doi.org/10.1089/jam.2007.0556.

Camm, A.J., Kirchhof, P., Lip, G.Y.H., Schotten, U., Savelieva, I., Ernst, S., Van Gelder, I. C., Al-Attar, N., Hindricks, G., Prendergast, B., Heidbuchel, H., Alfieri, O., Angelini, A., Atar, D., Colonna, P., De Caterina, R., De Sutter, J., Goette, A., Gorenek, B., Heldal, M., Hohloser, S.H., Kolh, P., Le Heuzey, J.Y., Ponikowski, P., Rutten, F.H., Vahanian, A., Auricchio, A., Bax, J., Ceconi, C., Dean, V., Filippatos, G., Funck-Brentano, C., Hobbs, R., Kearney, P., McDonagh, T., Popescu, B.A., Reiner, Z., Sechtem, U., Sirnes, P.A., Tendera, M., Vardas, P.E., Widimsky, P., Agladze, V., Aliot, E., Balabanski, T., Blomstrom-Lundqvist, C., Capucci, A., Crijns, H., Dahl?? f, B., Folliguet, T., Glikson, M., Goethals, M., Gulba, D.C., Ho, S.Y., Klautz, R.J.M., Kose, S., McMurray, J., Perrone Filardi, P., Raatikainen, P., Salvador, M.J., Schalij, M.J., Shpektor, A., Sousa, J., Stepinska, J., Uuetoa, H., Zamorano, J.L., Zupan, I., 2010. Guidelines for the management of atrial fibrillation. Eur. Heart J. 31, 2369–2429. https://doi.org/10.1093/eurheartj/ehq278.

Carrigy, N.B., Chang, R.Y., Leung, S.S.Y., Harrison, M., Petrova, Z., Pope, W.H., Hatfull, G.F., Britton, W.J., Chan, H.K., Sauvageau, D., Finlay, W.H., Vehring, R., 2017. Anti-tuberculosis bacteriophage D29 delivery with a vibrating mesh nebulizer, Jet Nebulizer, and Soft Mist Inhaler. Pharm. Res. 34, 2084–2096. https://doi.org/10.1007/s11095-017-2213-4.

Ceschan, N.E., Bucalá, V., Ramírez-Rigo, M.V., 2014. New alginic acid-atenolol microparticles for inhalatory drug targeting. Mater. Sci. Eng. C 41, 255–266. https://doi.org/10.1016/j.msec.2014.04.040.

Ceschan, N.E., Bucalá, V., Ramírez-Rigo, M.V., Smyth, H.D.C., 2016. Impact of feed counterion addition and cyclone type on aerodynamic behavior of alginic-atenolol microparticles produced by spray drying. Eur. J. Pharm. Biopharm. 109, 72–80. https://doi.org/10.1016/j.ejpb.2016.09.020.

Chen, X., Slättengren, T., Lange, E.C.M., Smith, D.E., Hammarlund-Udenaes, M., 2017. Revisiting atenolol as a low passive permeability marker. Fluids Barriers CNS 14, 1–14. https://doi.org/10.1186/s12987-017-0078-x.

Demou, J.S., Sidhom, M.B., Plakogiannis, F.M., 1994. Comparative in vitro diffusion studies for atenolol transdermal delivery system. Pharm. Acta Helv. 68, 215–219. https://doi.org/10.1016/0031-6865(94)90050-7.

Dong, W., Ye, J., Zhou, J., Wang, W., Wang, H., Zheng, X., Yang, Y., Xia, X., Liu, Y., 2020. Comparative study of mucoadhesive and mucus-penetrative nanoparticles based on phospholipid complex to overcome the mucus barrier for inhaled delivery of baicalein. Acta Pharm. Sin. B 10, 1576–1585. https://doi.org/10.1016/j.apsb.2019.10.002.

El-Assal, M.I.A., 2017. Proniosomes as nano-carrier for transdermal delivery of atenolol niosomal gel. Int. J. Drug Deliv. Technol. 7 https://doi.org/10.25258/ijddt.v7i04.10651.

Faragli, A., Oetvoes, J., Hohendanner, F., Primessnig, U., Pieske, B., Mühlfeld, C., Post, H., Heinzel, F.R., Iafisco, M., Catalucci, D., Alogna, A., 2021. Inhalation of peptide-loaded nanoparticles improves cardiac function in pacing-induced heart failure. Clin Res Cardiol. DGK Herztage. p. Abstract. https://doi.org/10.1007/s00392-021-01933-9.

Forbes, B., Ehrhardt, C., 2005. Human respiratory epithelial cell culture for drug delivery applications. Eur. J. Pharm. Biopharm. 60, 193–205. https://doi.org/10.1016/j.ejpb.2005.02.010.

Gallo, L., Bucalá, V., Ramírez-Rigo, M.V., 2017. Formulation and characterization of polysaccharide microparticles for pulmonary delivery of sodium cromoglycate. AAPS PharmSciTech 8, 1634–1645. https://doi.org/10.4103/0973-8398.84552.

Gallo, L., Llabot, J.M., Allemandi, D., Bucalá, V., Piña, J., 2011. Influence of spray-drying operating conditions on Rhamnus purshiana (Cáscara sagrada) extract powder physical properties. Powder Technol 208, 205–214. https://doi.org/10.1016/j.powtec.2010.12.021.

Gostick, N.K., Mayhew, S.R., Million, R., Sagar, D., Suxena, S.R., Ingram, D.F., Barmer, N. P., 1977. A dose-response study of atenolol in mild to moderate hypertension in general practice. Curr. Med. Res. Opin. 5, 179–184. https://doi.org/10.1185/03007997709110161.

Gupta, S.P., Jain, S.K., 2006. Transdermal atenolol releasing system: an approach towards its development. J. Drug Target. 14, 607–613. https://doi.org/10.1080/10611860600866591.

Gupta, S.P., Jain, S.K., 2004. Development of matrix-membrane transdermal drug delivery system for Atenolol. Drug Deliv. J. Deliv. Target. Ther. Agents 11, 281–286. https://doi.org/10.1080/10717540490493943.

Hariyadi, D.M., Islam, N., 2020. Current status of alginate in drug delivery. Adv. Pharmacol. Pharm. Sci 1–16. https://doi.org/10.1155/2020/8886095.

Hasnain, M.S., Guru, P.R., Rishishwar, P., Ali, S., Ansari, M.T., Nayak, A.K., 2020. Atenolol-releasing buccal patches made of Dillenia indica L. fruit gum: preparation and ex vivo evaluations. SN Appl. Sci. 2, 1–10. https://doi.org/10.1007/s42452-019-1756-x.

Islan, G.A., Ruiz, M.E., Morales, J.F., Sbaraglini, M.L., Enrique, A.V., Burton, G., Talevi, A., Bruno-Blanch, L.E., Castro, G.R., 2017. Hybrid inhalable microparticles for dual controlled release of levofloxacin and DNase: physicochemical characterization and in vivo targeted delivery to the lungs. J. Mater. Chem. B 5, 3132–3144. https://doi.org/10.1039/c6tb03366k.

Ivanovska, V., Rademaker, C.M.A., Van Dijk, L., Mantel-Teeuwisse, A.K., 2014. Pediatric drug formulations: a review of challenges and progress. Pediatrics 134, 361–372. https://doi.org/10.1542/peds.2013-3225.

Ivarsson, D., Wahlgren, M., 2012. Comparison of in vitro methods of measuring mucoadhesion: ellipsometry, tensile strength and rheological measurements. Colloids Surfaces B Biointerfaces 92, 353–359. https://doi.org/10.1016/j.colsurfb.2011.12.020.

Jaafar-Maalej, C., Diab, R., Andrieu, V., Elaissari, A., Fessi, H., 2010. Ethanol injection method for hydrophilic and lipophilic drug-loaded liposome preparation. J. Liposome Res. 20, 228–243. https://doi.org/10.3109/08982100903347923.

Jain, H., Bairagi, A., Srivastava, S., Singh, S.B., Mehra, N.K., 2020. Recent advances in the development of microparticles for pulmonary administration. Drug Discov. Today 25, 1865–1872. https://doi.org/10.1016/j.drudis.2020.07.018.

Johnson, J.C., Waldrep, J.C., Guo, J., Dhand, R., 2008. Aerosol delivery of recombinant human DNase I: in vitro comparison of a vibrating-mesh nebulizer with a jet nebulizer. Respir. Care 53, 1703–1708.

Kamali, H., Abbasi, S., Amini, M.A., Amani, A., 2016. Investigation of factors affecting aerodynamic performance of nebulized Nanoemulsion. Iran. J. Pharm. Res. 15, 687–693.

Khutoryanskiy, V., 2011. Advances in mucoadhesion and mucoadhesive polymers. Macromol. Biosci. 11, 748–764. https://doi.org/10.1002/mabi.201000388.

Kim, J., Shin, S.C., 2004. Controlled release of atenolol from the ethylene-vinyl acetate matrix. Int. J. Pharm. 273, 23–27. https://doi.org/10.1016/j.ijpharm.2003.12.004.

Kováčik, A., Kopečná, M., Vávrová, K., 2020. Permeation enhancers in transdermal drug delivery: benefits and limitations. Expert Opin. Drug Deliv. 17, 145–155. https://doi.org/10.1080/17425247.2020.1713087.

Lal, S., Datta, M., 2015. In vitro prolonged gastric residence and sustained release of atenolol using novel clay polymer nanocomposite. Appl. Clay Sci. 114, 412–421. https://doi.org/10.1016/j.clay.2015.06.017.

Mackie, A.R., Macierzanka, A., Aarak, K., Rigby, N.M., Parker, R., Channel, G.A., Harding, S.E., 2016. Sodium alginate decreases the permeability of intestinal mucus. Food Hydrocoll. Bajka, B.H., 52, 749–755. https://doi.org/10.1016/j.foodhyd.2015.08.004.

Mahler, D.A., Ohar, J.A., Barnes, C.N., Moran, E.J., Pendyala, S., Crater, G.D., 2019. Nebulized versus dry powder long-acting muscarinic antagonist bronchodilators in patients with COPD and suboptimal peak inspiratory flow rate. Chronic Obstr. Pulm. Dis. 6, 321–331. https://doi.org/10.15326/jcopdf.6.4.2019.0137.

Mimura, Y., Yasujima, T., Ohta, K., Inoue, K., Yuasa, H., 2017. Functional identification of plasma membrane monoamine transporter (PMAT/SLC29A4) as an atenolol transporter sensitive to flavonoids contained in apple juice. J. Pharm. Sci. 106, 2592–2598. https://doi.org/10.1016/j.xphs.2017.01.009.

Miragoli, M., Ceriotti, P., Iafisco, M., Vacchiano, M., Salvarani, N., Alogna, A., Carullo, P., Ramirez-Rodríguez, G.B., Patrício, T., Degli Esposti, L., Rossi, F., Ravanetti, F., Pinelli, S., Alinovi, R., Erreni, M., Rossi, S., Condorelli, G., Post, H., Tampieri, A., Catalucci, D., 2018. Inhalation of peptide-loaded nanoparticles improves heart failure. Sci. Transl. Med. 10, 1–12. https://doi.org/10.1126/scitranslmed.aan6205.

Mitchell, J., Newman, S., Chan, H., 2007. In vitro and in vivo aspects of cascade impactor tests and inhaler performance : a review. AAPS PharmSciTech 8, 237–248.

Moebus, K., Siepmann, J., Bodmeier, R., 2012. Novel preparation techniques for alginate – poloxamer microparticles controlling protein release on mucosal surfaces. Eur. J. Pharm. Sci. 45, 358–366. https://doi.org/10.1016/j.ejps.2011.12.004.

Mohanty, C., Subrahmanyam, K.V., 2017. Effect of sintering condition on physio-chemical parameters and drug release characteristics from polymeric matrix tablet of atenolol for controlled release. Int. J. Pharm. Sci. Res. 8, 3758–3767. https://doi.org/10.13040/IJPSR.0975-8232.8(9).3758-67.

Mortazavi-Derazkola, S., Salavati-Niasari, M., Khojasteh, H., Amiri, O., Ghoreishi, S.M., 2017. Green synthesis of magnetic Fe3O4/SiO2/HAp nanocomposite for atenolol

delivery and in vivo toxicity study. J. Clean. Prod. 168, 39–50. https://doi.org/10.1016/j.jclepro.2017.08.235.
Mundargi, R.C., Patil, S., Agnihotri, S., Aminabhavi, T.M., 2007. Evaluation and controlled release characteristics of modified xanthan films for transdermal delivery of atenolol. Drug Dev. Ind. Pharm. 33, 79–90. https://doi.org/10.1080/03639040600975030.
Netsomboon, K., Bernkop-Schnürch, A., 2016. Mucoadhesive vs. mucopenetrating particulate drug delivery. Eur. J. Pharm. Biopharm. 98, 76–89. https://doi.org/10.1016/j.ejpb.2015.11.003.
Newman, S.P., Chan, H.K., 2008. In vitro/in vivo comparisons in pulmonary drug delivery. J. Aerosol Med. Pulm. Drug Deliv. 21, 77–84. https://doi.org/10.1089/jamp.2007.0643.
Nimon, K.F., 2012. Statistical assumptions of substantive analyses across the general linear model: a mini-review. Front. Psychol. 3, 1–5. https://doi.org/10.3389/fpsyg.2012.00322.
Nordgård, C.T., Nonstad, U., Olderøy, M., Espevik, T., Draget, K.I., 2014. Alterations in mucus barrier function and matrix structure induced by guluronate oligomers. Biomacromolecules 15, 2294–2300. https://doi.org/10.1021/bm500464b.
Olivera, M.E., Manzo, R., Alovero, F., Jimenez-Kairuz, A.f., Ramírez-Rigo, M.V., 2017. Polyelectrolyte-drug ionic complexes as nanostructured drug carriers to design solid and liquid oral delivery systems. In: Andronescu, E., Grumezescu, A.M. (Eds.), Nanostructures For Oral Medicine, Eds. Elsevier, pp. 365–408.
Ong, H.X., Traini, D., Bebawy, M., Young, P.M., 2011. Epithelial profiling of antibiotic controlled release respiratory formulations. Pharm. Res. 28, 2327–2338. https://doi.org/10.1007/s11095-011-0462-1.
Palazzo, F., Giovagnoli, S., Schoubben, A., Blasi, P., Rossi, C., Ricci, M., 2013. Development of a spray-drying method for the formulation of respirable microparticles containing ofloxacin-palladium complex. Int. J. Pharm. 440, 273–282. https://doi.org/10.1016/j.ijpharm.2012.05.045.
Pham, D.T., Chokamonsirikun, A., Phattaravorakarn, V., Tiyaboonchai, W., 2021. Polymeric micelles for pulmonary drug delivery: a comprehensive review. J. Mater. Sci. 56, 2016–2036. https://doi.org/10.1007/s10853-020-05361-4.
Poli, G., Acerbi, D., Pennini, R., Soliani-Raschini, A., Corrado, M.E., Eichler, H.G., Eichler, I., 2007. Clinical pharmacology study of Bramitob, a tobramycin solution for nebulization, in comparison with Tobi. Pediatr. Drugs 9, 3–9.
Rabinowitz, J.D., Zaffaroni, A.C., 2006. Delivery of Beta-blockers through an inhalation route. 7,048,909 B2.
Radwan, S.E.S., Sokar, M.S., Abdelmonsif, D.A., El-Kamel, A.H., 2017. Mucopenetrating nanoparticles for enhancement of oral bioavailability of furosemide: in vitro and in vivo evaluation/sub-acute toxicity study. Int. J. Pharm. 526, 366–379. https://doi.org/10.1016/j.ijpharm.2017.04.072.
Ramırez Rigo, M.V., Allemandi, D.A., Manzo, R.H., 2006. Swellable drug–polyelectrolyte matrices (SDPM) of alginic acid Characterization and delivery properties. Int. J. Pharm. 322, 36–44.
Ramkanth, S., Chetty, C.M., Sudhakar, Y., Thiruvengadarajan, V.S., Anitha, P., Gopinath, C., 2018. Development, characterization & invivo evaluation of proniosomal based transdermal delivery system of Atenolol. Futur. J. Pharm. Sci. 4, 80–87. https://doi.org/10.1016/j.fjps.2017.10.003.
Razavi Rohani, S.S., Abnous, K., Tafaghodi, M., 2014. Preparation and characterization of spray-dried powders intended for pulmonary delivery of insulin with regard to the selection of excipients. Int. J. Pharm. 465, 464–478. https://doi.org/10.1016/j.ijpharm.2014.02.030.
Rowe, R.C., Sheskey, P.J., Quinn, M., Armstrong, N., Rowe, R.C., Sheskey, P.J., Quinn, M., 2009. Alginic Acid. In: Rowe, R., Sheskey, P., Quinn, M. (Eds.), Handbook of Pharmaceutical Excipients 6th Ed, Eds. Pharmaceutical Press and Americal Pharmacist Association, London, pp. 20–22. https://doi.org/10.1016/0168-3659(95)00170-0.
Séchoy, O., Tissié, G., Sébastian, C., Maurin, F., Driot, J.-Y.Y., Trinquand, C., 2000. A new long acting ophthalmic formulation of Carteolol containing alginic acid. Int. J. Pharm. 207, 109–116. https://doi.org/10.1016/S0378-5173(00)00539-1.
Shin, S.C., Choi, J.S., 2003. Enhanced bioavailability of atenolol by transdermal administration of the ethylene-vinyl acetate matrix in rabbits. Eur. J. Pharm. Biopharm. 56, 439–443. https://doi.org/10.1016/S0939-6411(03)00133-4.
Singh, B., Chakkal, S.K., Ahuja, N., 2006. Formulation and optimization of controlled release mucoadhesive tablets of atenolol using response surface methodology. AAPS Pharm.Sci.Tech. 7, 1–10. https://doi.org/10.1208/pt070103.
Soares, J.P., Santos, J.E., Chierice, G.O., Cavalheiro, E.T.G., 2004. Thermal behavior of alginic acid and its sodium salt. Eclética Química 29, 57–64. https://doi.org/10.1590/S0100-46702004000200009.
Suárez Landazábal, O., Villarreal Sotomayor, C., Parody Muñoz, A., Rodríguez Delgado, A., Rebolledo Cobos, R., 2019. Prevalence of arterial hypertension and its risk factors in university students from Barranquilla, Colombia. Rev. la Fac. Ciencias la Salud Univ. del Cauca 21, 16–23. https://doi.org/10.47373/rfcs.2019.v21.1372.
Surber, M.W., Bostian, K.A., Dudley, M.N., Lomovskaya, O., Griffith, D.C., 2010. Aerosolized fluoroquinolones and uses thereof. US 7,838,532 B2.
Taffet, G.E., Donohue, J.F., Altman, P.R., 2014. Clinical Interventions in Aging Dovepress Considerations for managing chronic obstructive pulmonary disease in the elderly. Clin. Interv. Aging 9, 23–30.
Tanner, T., Marks, R., 2008. Delivering drugs by the transdermal route: review and comment. Ski. Res. Technol. 14, 249–260. https://doi.org/10.1111/j.1600-0846.2008.00316.x.
Todo, H., 2017. Transdermal permeation of drugs in various animal species. Pharmaceutics 9, 1–11. https://doi.org/10.3390/pharmaceutics9030033.
Tontul, I., Topuz, A., 2017. Spray-drying of fruit and vegetable juices: effect of drying conditions on the product yield and physical properties. Trends Food Sci. Technol. 63, 91–102. https://doi.org/10.1016/j.tifs.2017.03.009.
Traini, D., 2013. Inhalation drug delivery. In: Colombo, P., Traini, D., Buttini, F. (Eds.), Inhalation Drug Delivery: Techniques and Products, Eds. John Wiley & Sons, Ltd, pp. 1–14. https://doi.org/10.1002/9781118397145.ch1.
Traini, D., Young, P.M., 2009. Delivery of antibiotics to the respiratory tract: an update. Expert Opin. Drug Deliv. 6, 897–905. https://doi.org/10.1517/17425240903110710.
Ungaro, F., D'Angelo, I., Coletta, C., D'Emmanuele Di Villa Bianca, R., Sorrentino, R., Perfetto, B., Tufano, M.A., Miro, A., La Rotonda, M.I., Quaglia, F., 2012a. Dry powders based on PLGA nanoparticles for pulmonary delivery of antibiotics: modulation of encapsulation efficiency, release rate and lung deposition pattern by hydrophilic polymers. J. Control. Release 157, 149–159. https://doi.org/10.1016/j.jconrel.2011.08.010.
Ungaro, F., D'Angelo, I., Miro, A., La Rotonda, M.I., Quaglia, F., 2012b. Engineered PLGA nano- and micro-carriers for pulmonary delivery: challenges and promises. J. Pharm. Pharmacol. 64, 1217–1235. https://doi.org/10.1111/j.2042-7158.2012.01486.x.
USP38-NF33, 2015. <1601>Products for nebulization—characterization tests. The United States Pharmacopeia-The National Formulary. The United States Pharmacopeial Convention, Rockville, pp. 1610–1613.
Verma, R., Ibrahim, M., Garcia-Contreras, L., 2015. Lung anatomy and physiology and their implications for pulmonary drug delivery. In: Nokhodchi, A., Martin, G. (Eds.), Pulmonary Drug Delivery: Advances and Challenges, Eds. John Wiley & Sons, pp. 1–18.
Videira, M.A., Llop, J., Sousa, C., Kreutzer, B., Cossío, U., Forbes, B., Vieira, I., Gil, N., Silva-Lima, B., 2020. Pulmonary administration: strengthening the value of therapeutic proximity. Front. Med. 7, 1–11. https://doi.org/10.3389/fmed.2020.00050.
Villanueva, N.D.M., Petenate, A.J., Da Silva, M.A.A.P., 2000. Performance of three affective methods and diagnosis of the ANOVA model. Food Qual. Prefer. 11, 363–370. https://doi.org/10.1016/S0950-3293(00)00006-9.
Wesolowski, M., Rojek, B., 2013. Thermogravimetric detection of incompatibilities between atenolol and excipients using multivariate techniques. J. Therm. Anal. Calorim. https://doi.org/10.1007/s10973-013-3070-y.
Xue, Y., Yu, S., Wang, H., Liang, J., Peng, J., Li, J., Yang, X., Pan, W., 2015. Design of a timed and controlled release osmotic pump system of atenolol. Drug Dev. Ind. Pharm. 41, 906–915. https://doi.org/10.3109/03639045.2014.913612.
Yang, Y., Faustino, P.J., Volpe, D.A., Ellison, C.D., Lyon, R.C., Yu, L.X., 2007. Biopharmaceutics Classification of Selected β-blockers: solubility and permeability class membership. Mol. Pharm. 4, 608–614. https://doi.org/10.1021/mp070028i.
Yeh, H.C., Schum, G.M., 1980. Models of human lung airways and their applicatioon to inhaled particle deposition. Bull. Math. Biol. 42, 461–480.
Yusuf, S., Joseph, P., Rangarajan, S., Islam, S., Mente, A., Hystad, P., Brauer, M., Kutty, V. R., Gupta, R., Wielgosz, A., AlHabib, K.F., Dans, A., Lopez-Jaramillo, P., Avezum, A., Lanas, F., Oguz, A., Kruger, I.M., Diaz, R., Yusoff, K., Mony, P., Chifamba, J., Yeates, K., Kelishadi, R., Yusufali, A., Khatib, R., Rahman, O., Zatonska, K., Iqbal, R., Wei, L., Bo, H., Rosengren, A., Kaur, M., Mohan, V., Lear, S.A., Teo, K.K., Leong, D., O'Donnell, M., McKee, M., Dagenais, G., 2020. Modifiable risk factors, cardiovascular disease, and mortality in 155 722 individuals from 21 high-income, middle-income, and low-income countries (PURE): a prospective cohort study. Lancet 395, 795–808. https://doi.org/10.1016/S0140-6736(19)32008-2.